



ME-446: Liquid-gas interfacial heat and mass transfer

Flow Boiling

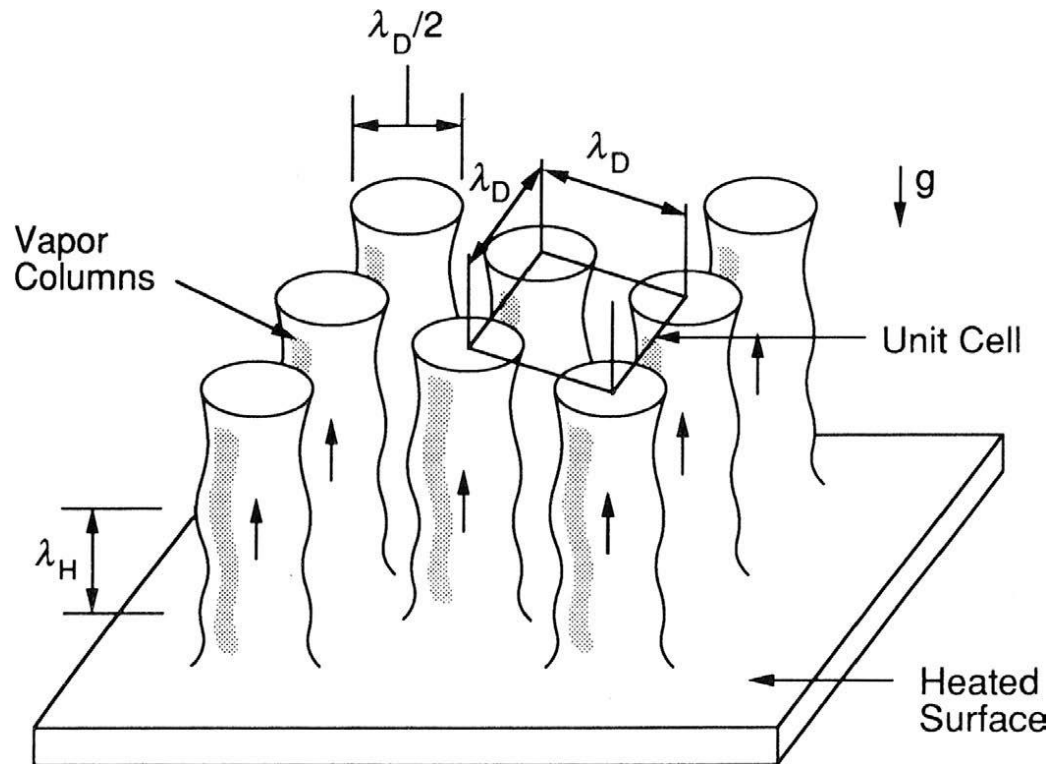
Zhengmao Lu
Energy Transport Advances
Laboratory
EPFL Mechanical Engineering

2025 Fall Semester

Photo Credit: Trougnouf

- Zuber' CHF model based on hydrodynamic instability
- Force balance model for CHF
- Statistical approach for CHF

$$u_c = \sqrt{\frac{2\pi\sigma}{\rho_v\lambda_D}} \quad \lambda_H = \lambda_D = 2\pi\sqrt{\frac{3\sigma}{\Delta\rho g}}$$



$$u_c = \frac{q''_{max}}{\rho_v h_{lv}} \left(\frac{A_{surf}}{A_{col}} \right) = \frac{16 q''_{max}}{\pi \rho_v h_{lv}}$$

$$q''_{max} = 0.149 \rho_v h_{lv} \left(\frac{\sigma \Delta \rho g}{\rho_v^2} \right)^{1/4}$$

$$q_K'' = \rho_v h_{fg} \left(\frac{1 + \cos \beta}{16} \right) \left[\frac{2}{\pi} + \frac{\pi}{4} (1 + \cos \beta) \right]^{\frac{1}{2}} \left(\frac{\sigma \Delta \rho g}{\rho_v^2} \right)^{\frac{1}{4}} \quad (\text{Horizontal surface})$$

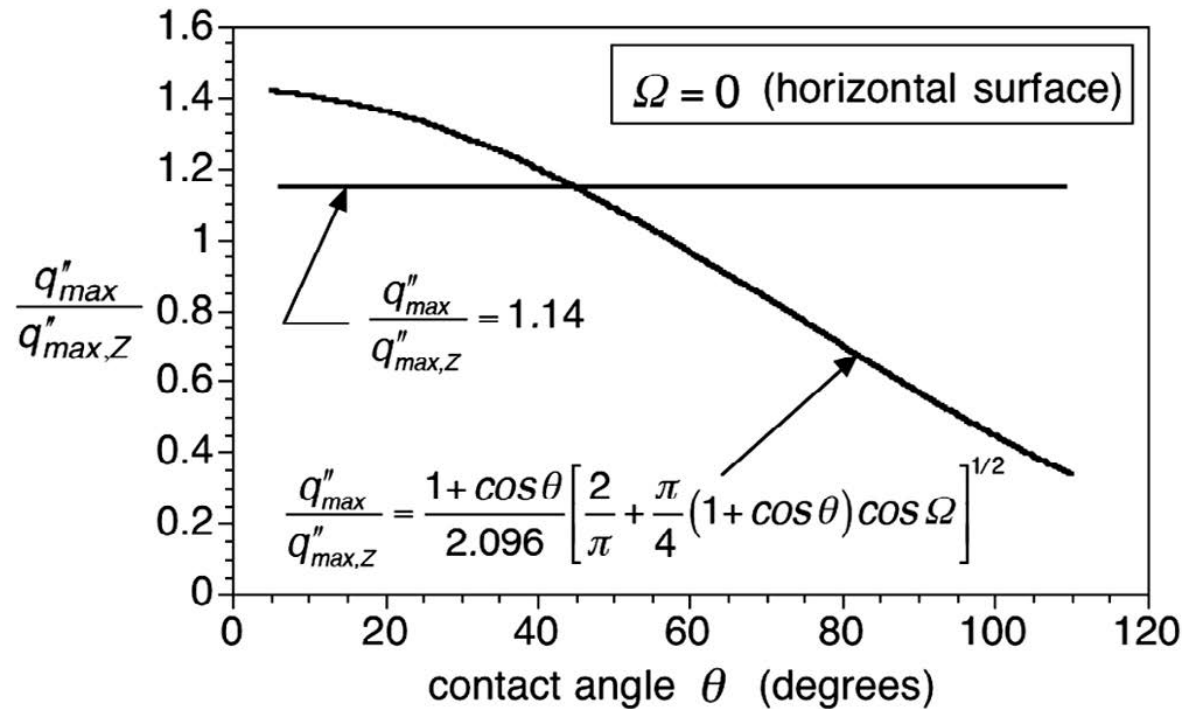


FIGURE 7.19 in Carey

$$q''_{max,Z} = 0.149 \rho_v h_{lv} \left(\frac{\sigma \Delta \rho g}{\rho_v^2} \right)^{\frac{1}{4}}$$

$$\frac{q_K''}{q''_{max,Z}} = \frac{1 + \cos \theta}{2.096} \left[\frac{2}{\pi} + \frac{\pi}{4} (1 + \cos \beta) \right]^{\frac{1}{2}}$$

- Isolated bubbles dissipate heat better than merged bubbles
- CHF is reached when you have the **maximum number** of isolated bubbles
- With elevated temperature, 1) more nucleation sites become activated while 2) more bubbles are likely to merge into each other.

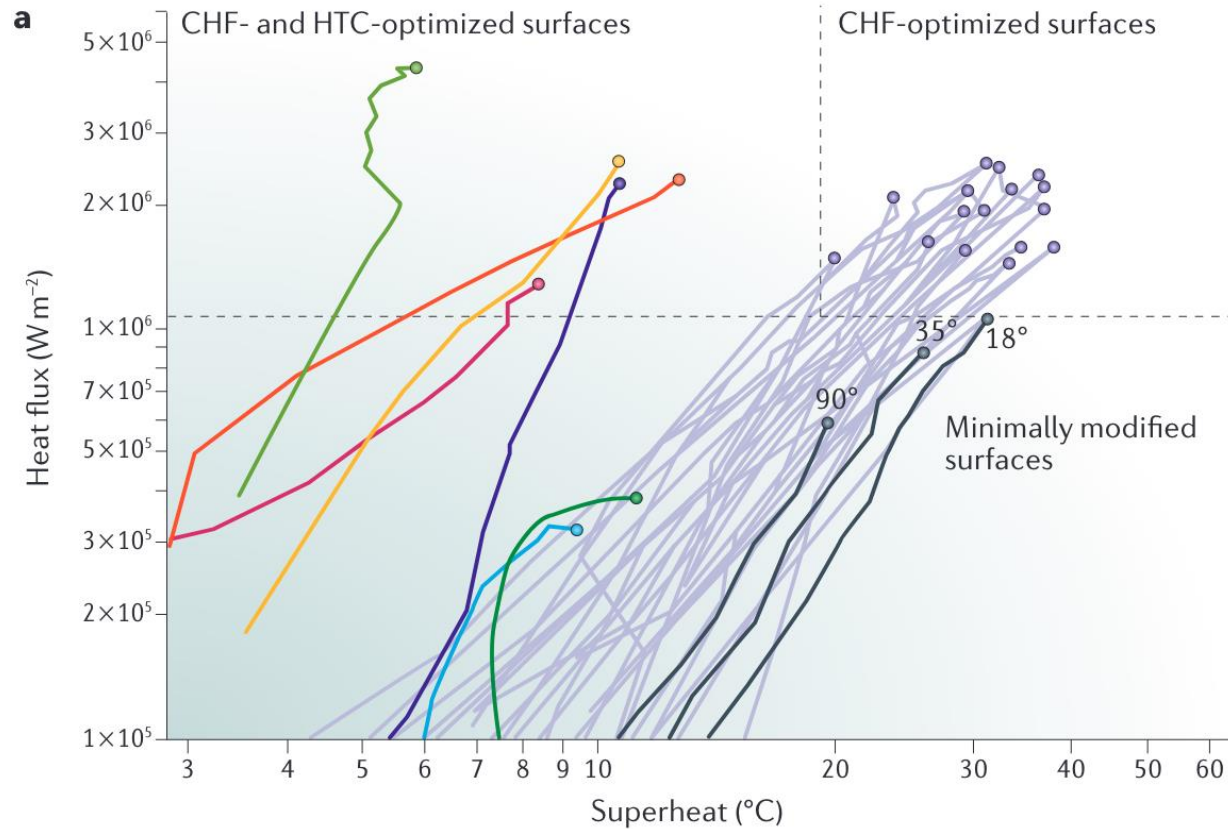
$$\frac{\partial N_{iso}}{\partial T} = 0$$

$$\frac{\partial}{\partial T} \left[\sum_{N=1}^{\infty} \frac{N_0^N}{(N-1)!} \exp \left(-N_0 - \frac{\pi N D_b^2}{A} \right) \right] = 0$$

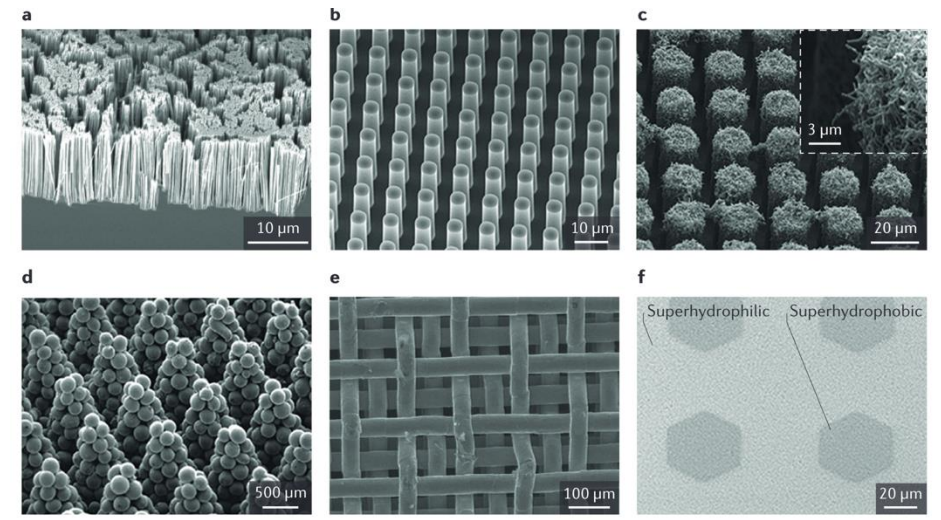
$$\Rightarrow n_0 \pi D_b^2 = 1$$

A unified relationship between the nucleation density at CHF and bubble diameter

- Understand how wicking surfaces enhance CHF
- Know different flow boiling regimes
- Evaluate ONB, HTC, and CHF in flow boiling with correlations

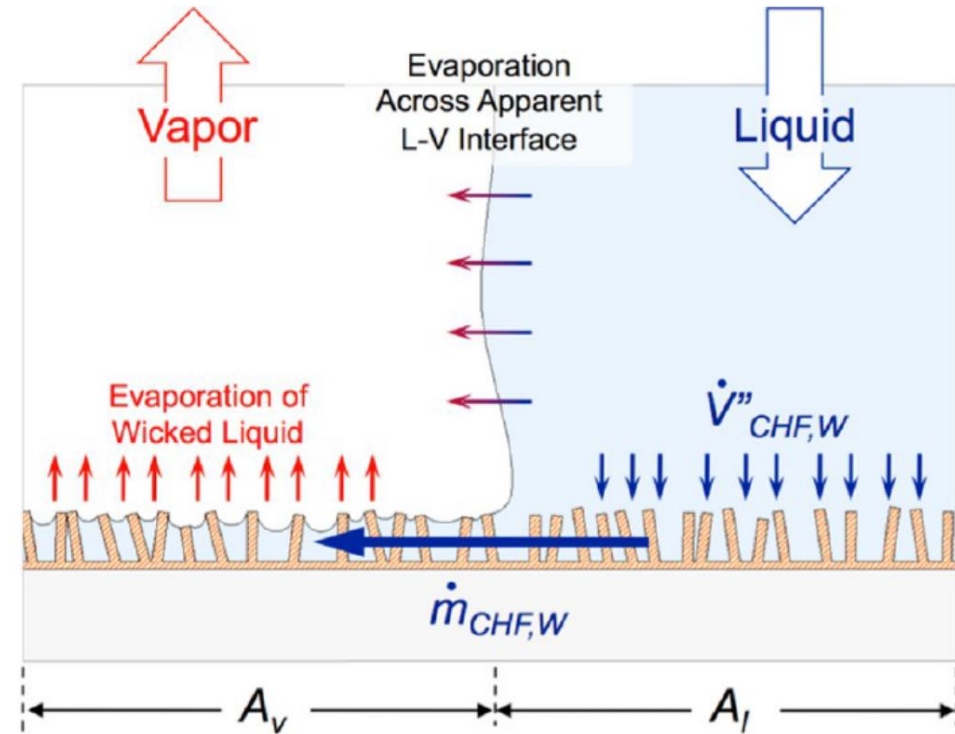
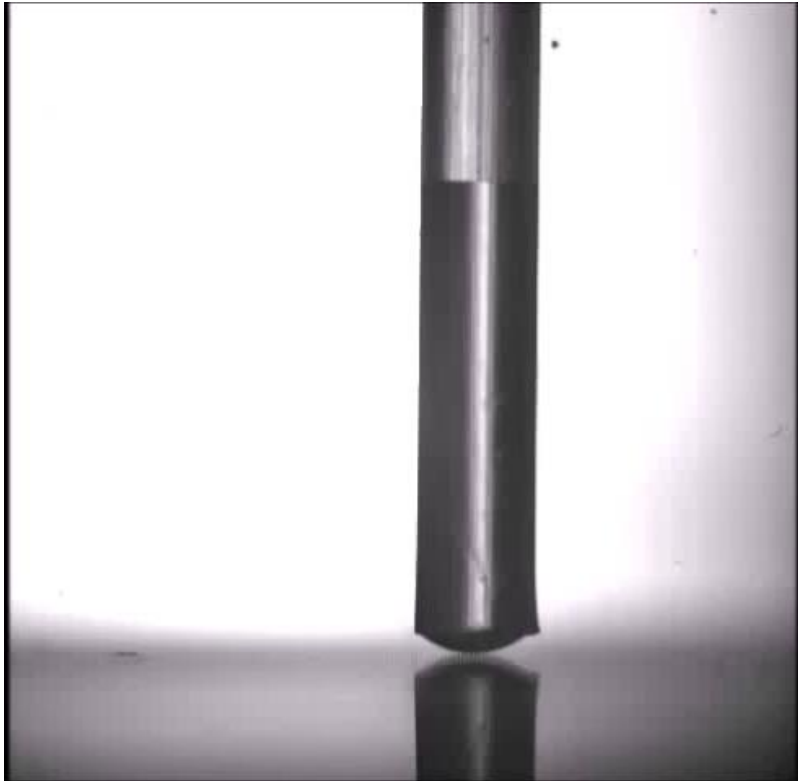
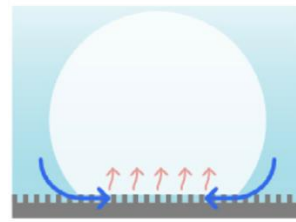


- Sintered microchannels¹³¹
- Sintered wire mesh¹²⁵
- Microchannels¹³⁰
- Biconductive¹²⁹
- Superbiphilic¹²⁸
- Surfactant desorbed¹³⁵
- Surfactant adsorbed¹³⁵
- Hydrophilic micro- and nanostructured (structured, porous and nanofluid)^{34,35,37,39,40,42,43}
- 18° smooth²⁰
- 35° smooth²⁰
- 90° smooth²⁰



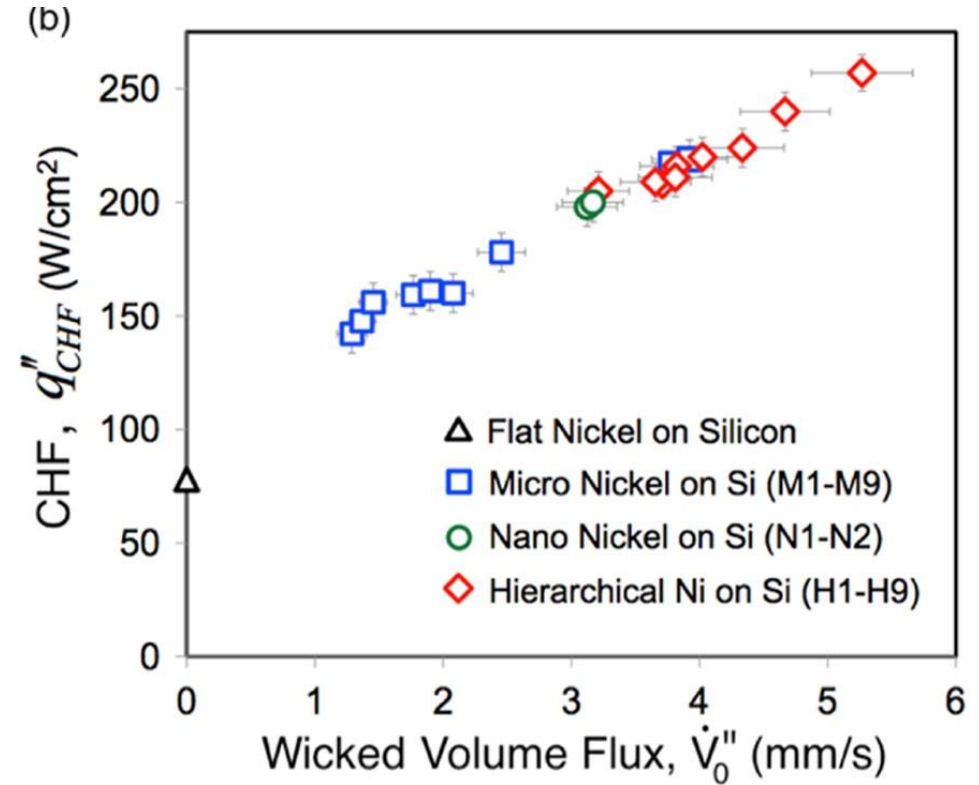
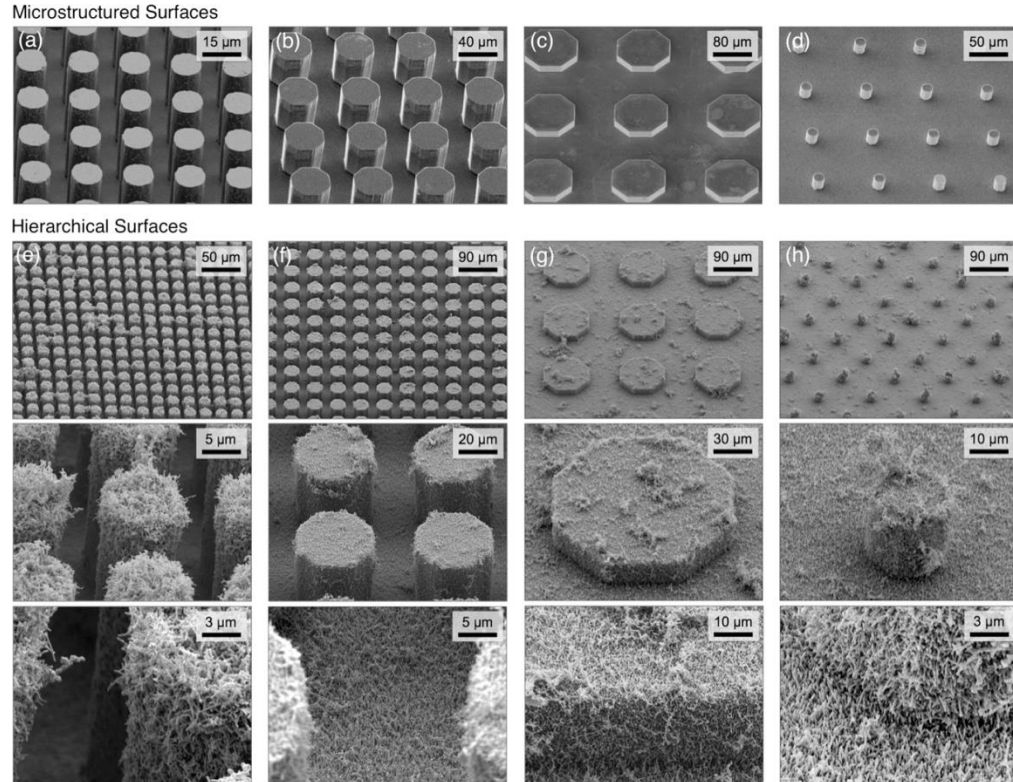
doi:10.1038/natrevmats.2016.92

Wicking Helps Boiling



<https://doi.org/10.1021/acs.langmuir.7b01522>

<https://doi.org/10.1021/la5030923>



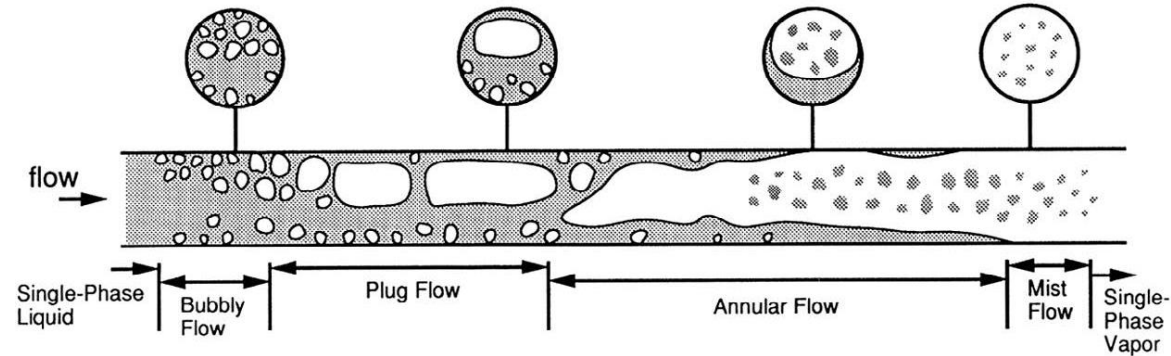
<https://doi.org/10.1021/la5030923>

Summary on Boiling CHF

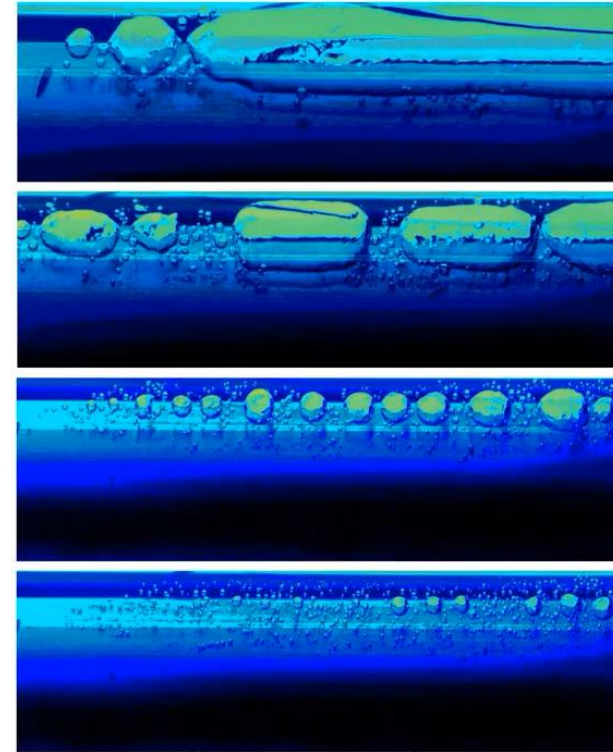
- On flat surfaces, CHF is thought to be caused by 1) hydrodynamic instabilities and/or 2) number of isolated bubbles reaching maximum
- With wicking surfaces, additional liquid supply (through capillarity) to the bubble can improve CHF

What is Flow Boiling

Different regimes in flow boiling

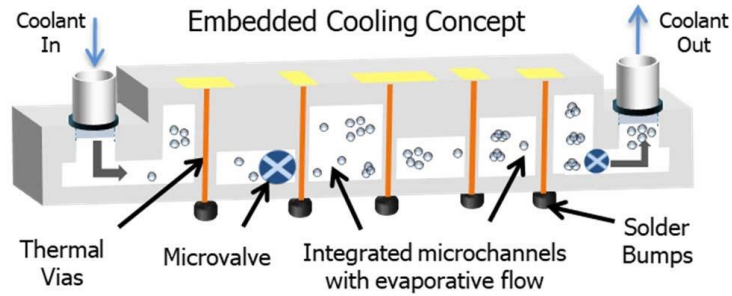


Flow boiling: boiling where forced convection is employed to replenish the boiling liquid and push developed vapors downstream

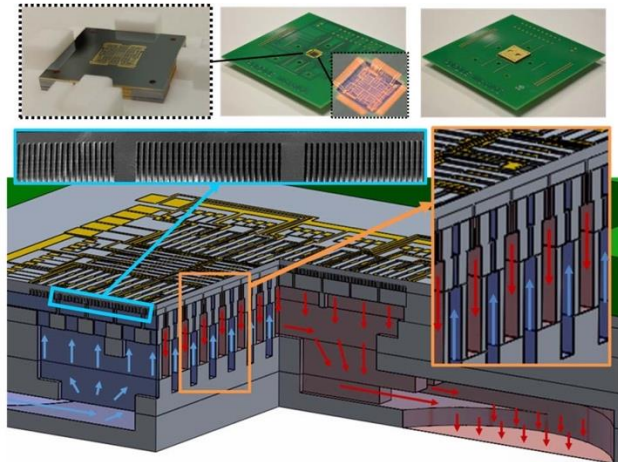


Videos slowed down 50 times

High flux electronics cooling



IEEE TCPMT 11.10 (2021): 1546-1564.

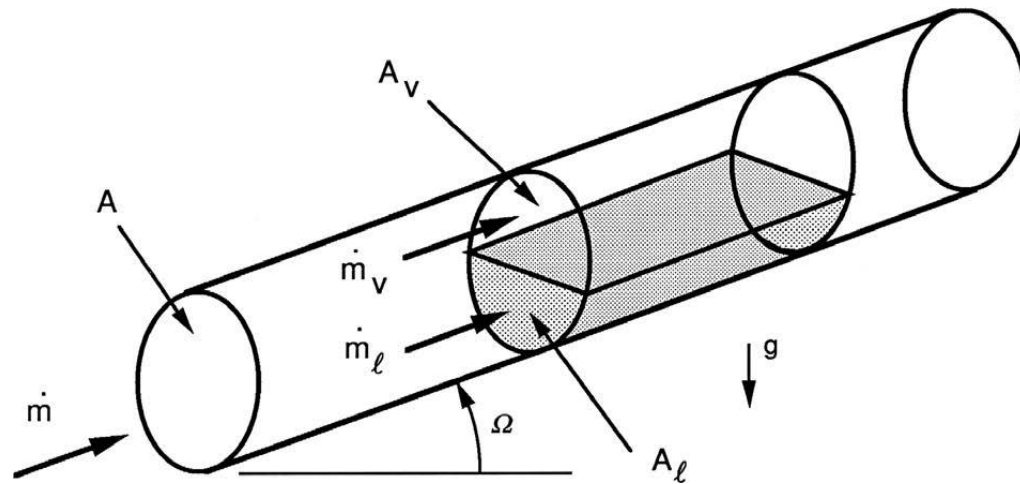


IJHMT 117 (2018) 319–330

Nuclear reactors



Credit: Tennessee Valley Authority



Idealized model for defining flow properties
Figure 10.1 in Carey

Total mass flow rate

$$\dot{m} = \dot{m}_v + \dot{m}_l$$

Vapor quality

$$x = \dot{m}_v / \dot{m}$$

Mass velocity

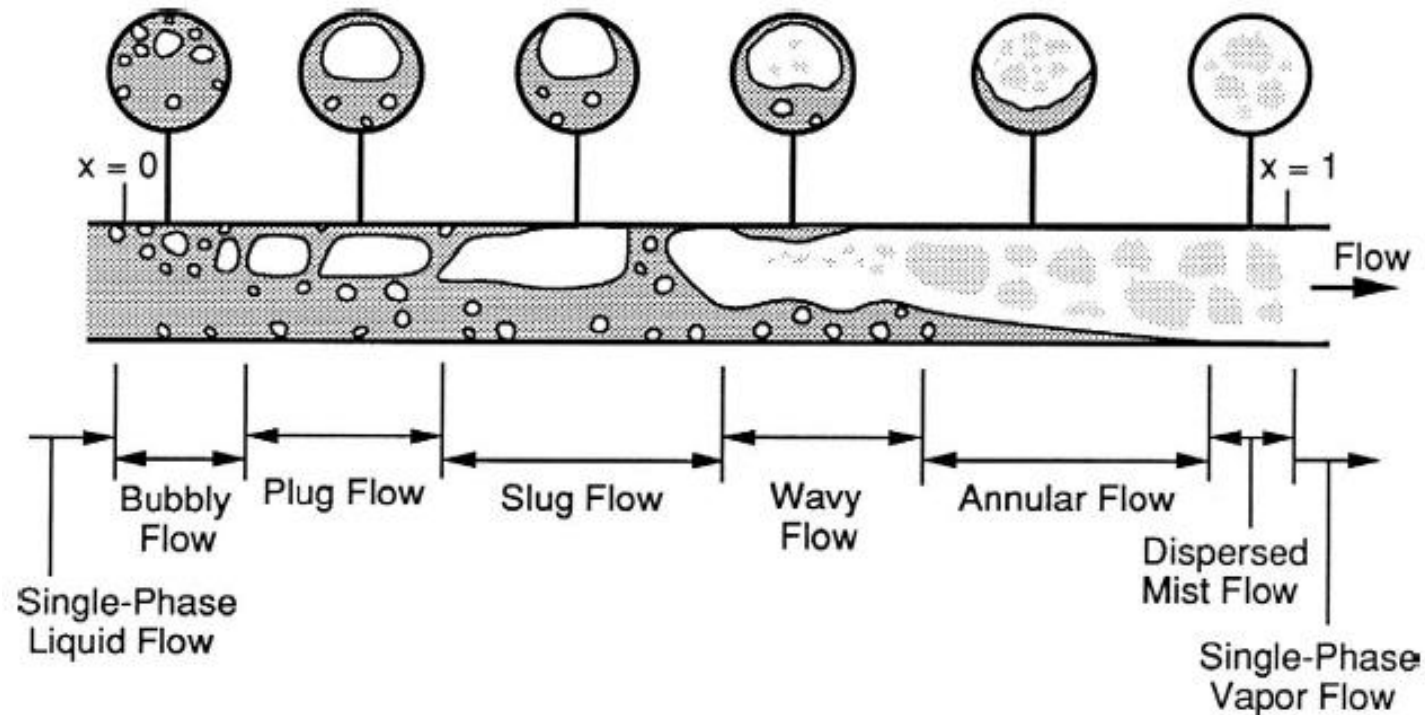
$$G = \dot{m} / A$$

Vapor volume flux $j_v = Gx / \rho_v$

Liquid volume flux $j_l = G(1 - x) / \rho_l$

Void fraction $\alpha = A_v / A$

Flow Regimes (Horizontal Tubes)



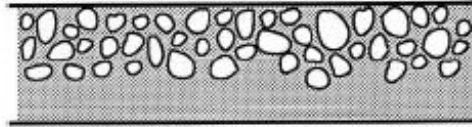
Liquid enters the tube subcooled

After onset of nucleation:

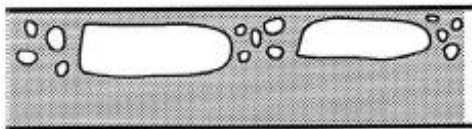
- Bubbly flow
- Plug flow
- Slug flow
- Stratified flow
- Wavy flow
- Annular flow
- Mist flow

Figure 10.8 in Carey

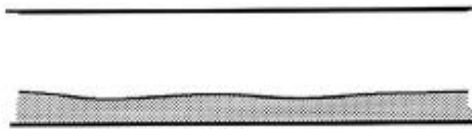
Flow Regimes (Horizontal Tubes)



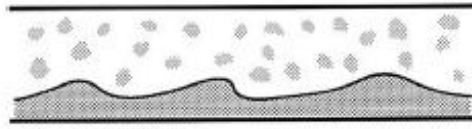
Bubbly flow: discrete bubbles dispersed in continuous liquid phase



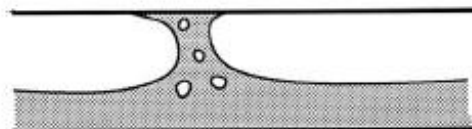
Plug flow: coalescence of small bubbles produces larger bubbles flowing in the upper portion



Stratified flow: liquid flowing in the bottom of the pipe is separated from vapor in the upper portion of the pipe by a relatively smooth interface (low flow rate, relatively high quality)



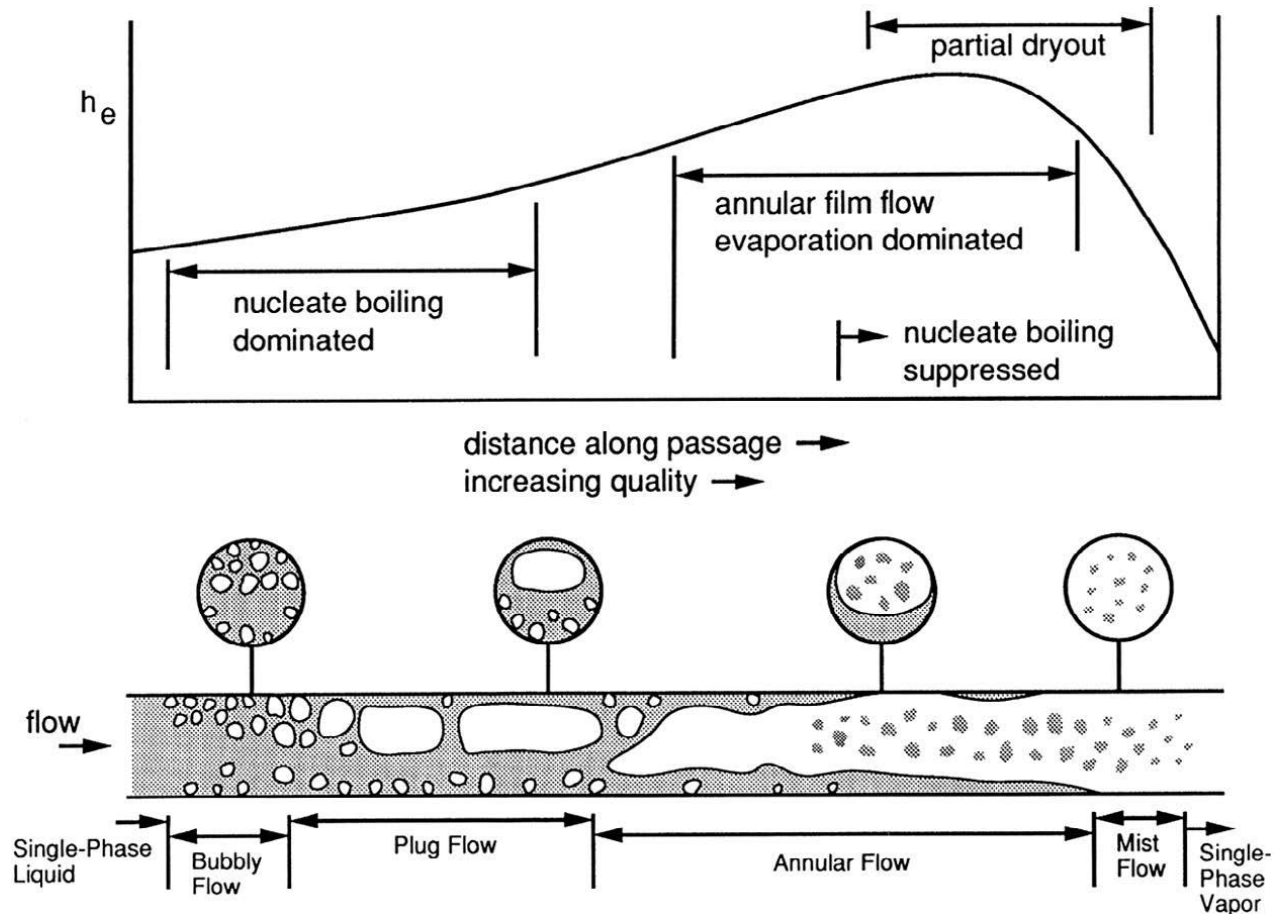
Wavy flow: continuous vapor core, continuous but disturbed liquid film on wall (Helmholtz instability), often with entrainment of droplets



Slug flow: slugs of vapor flowing along the tube toward the upper portion

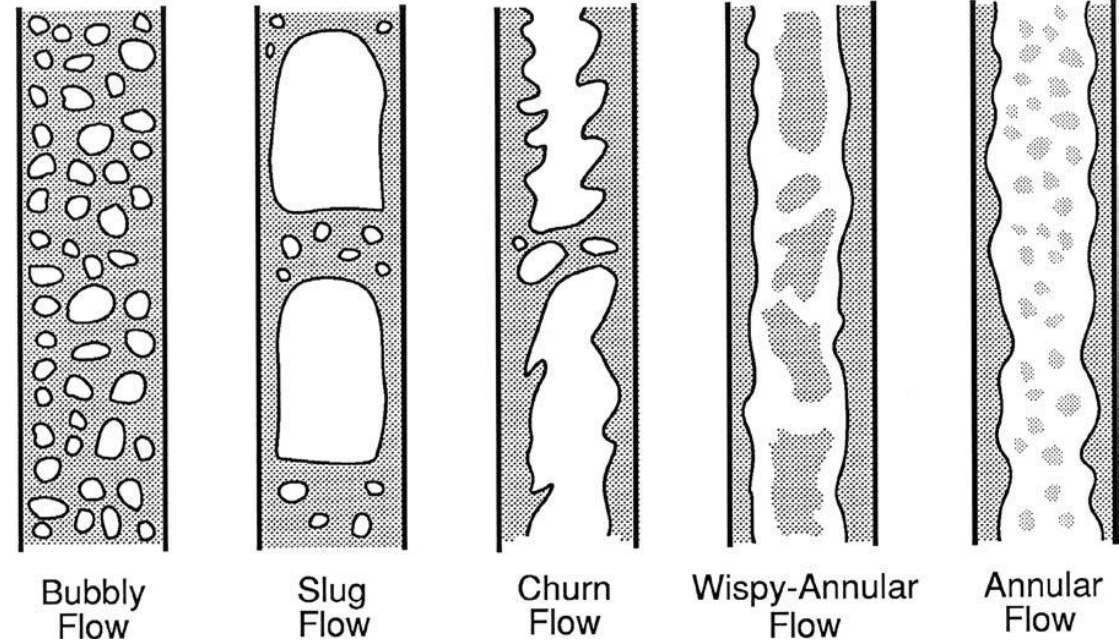
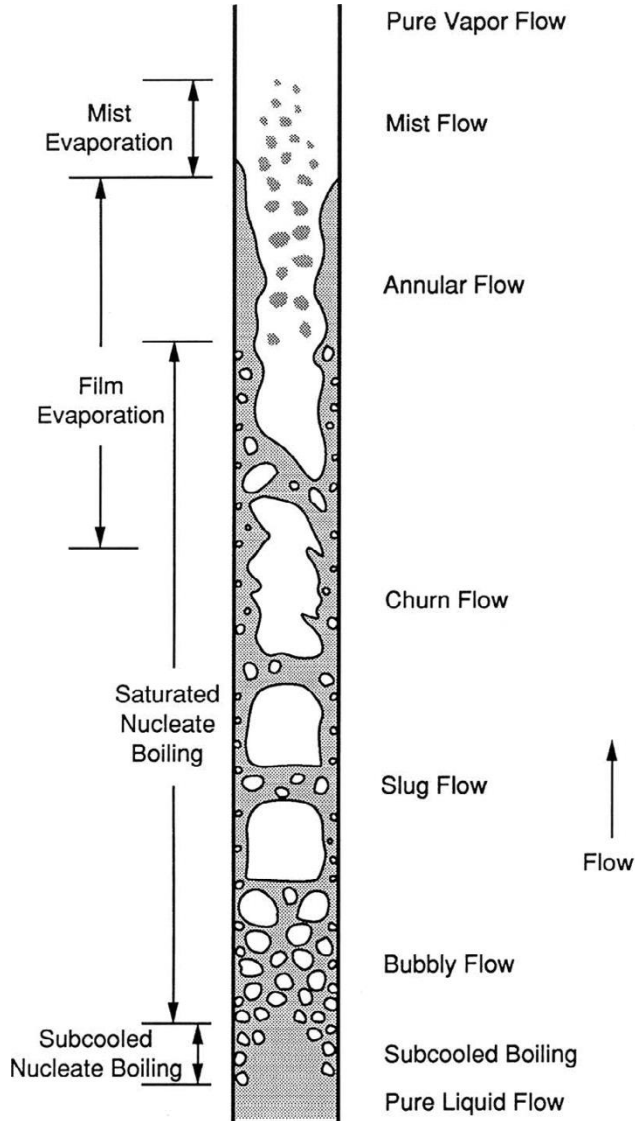


Annular flow: most liquid flowing along the wall and gas flowing in the central core, in an annular configuration with entrainment of droplets. When the liquid film dries out, it becomes **mist flow**



- HTC increases after onset of nucleation and decreases as dryout occurs
- Annular flow provides best HTC

Flow Regimes (Upflow Vertical Tube)

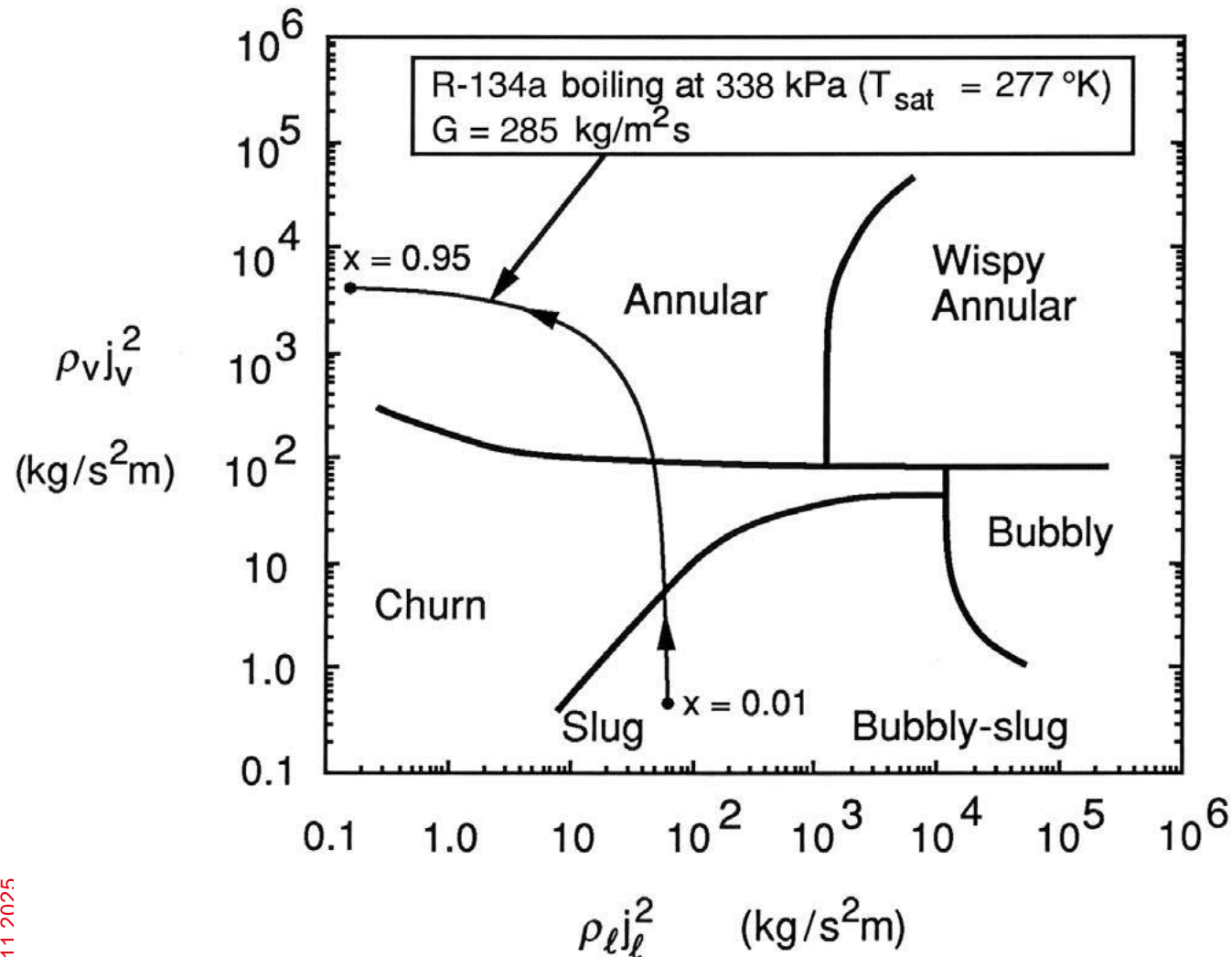


More axisymmetric than horizontal tubes

Churn flow: large bubbles with unstable, oscillatory, irregular interfaces

Wispy-annular flow: annular flow with heavy “wisps” (both liquid and vapor flow rates are high)

Hewitt and Roberts Flow Regime Map



Vapor volume flux $j_v = Gx/\rho_v$

Liquid volume flux $j_l = G(1 - x)/\rho_l$

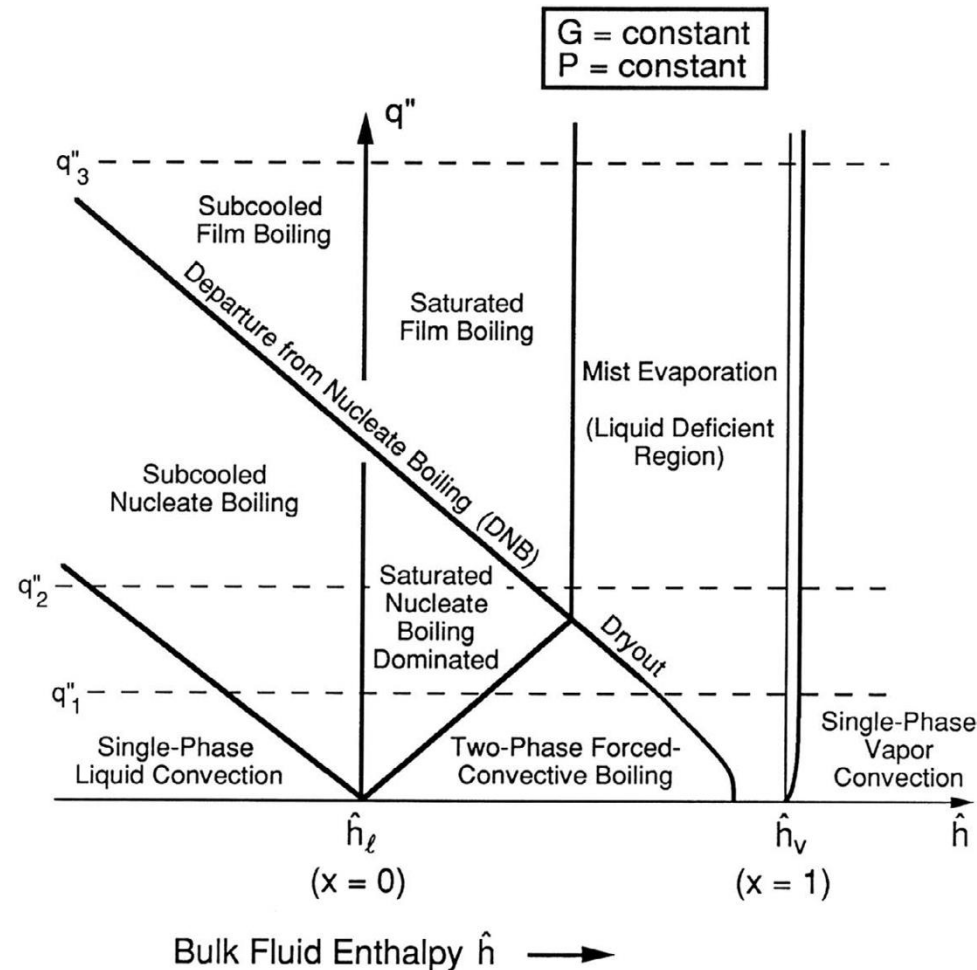
x-axis: momentum flux of liquid

y-axis: momentum flux of vapor

Curve A: constant mass flux

$$\rho_v j_v + \rho_l j_l = G$$

Depends on tube configuration, working fluids, and working conditions

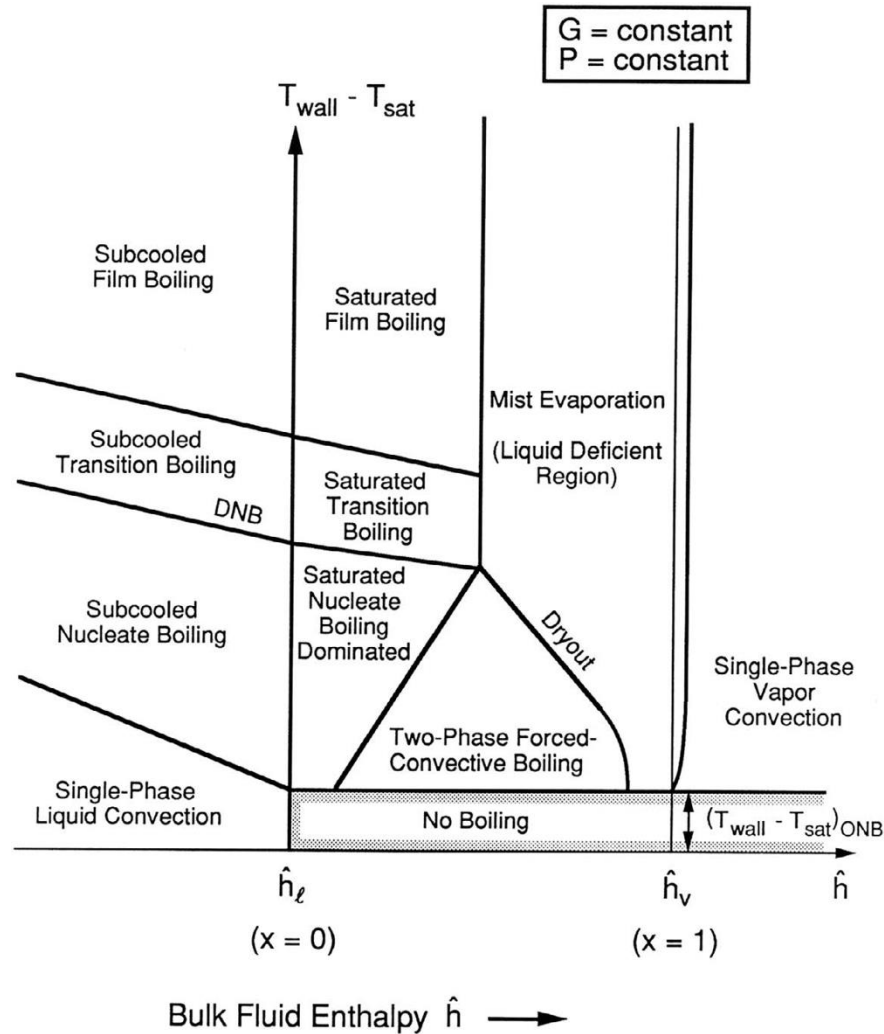


Low heat fluxes q''_1 :
 subcooled liquid \rightarrow subcooled boiling \rightarrow saturated boiling
 dominated \rightarrow convective flow boiling \rightarrow mist evaporation
 \rightarrow pure vapor

Intermediate heat fluxes q''_2 :
 subcooled liquid \rightarrow subcooled boiling \rightarrow saturated boiling
 dominated \rightarrow film boiling \rightarrow mist evaporation \rightarrow pure vapor

High heat fluxes q''_3 :
 subcooled liquid \rightarrow (subcooled and saturated) film boiling
 \rightarrow mist evaporation \rightarrow pure vapor

Boiling Regimes with Isothermal Wall



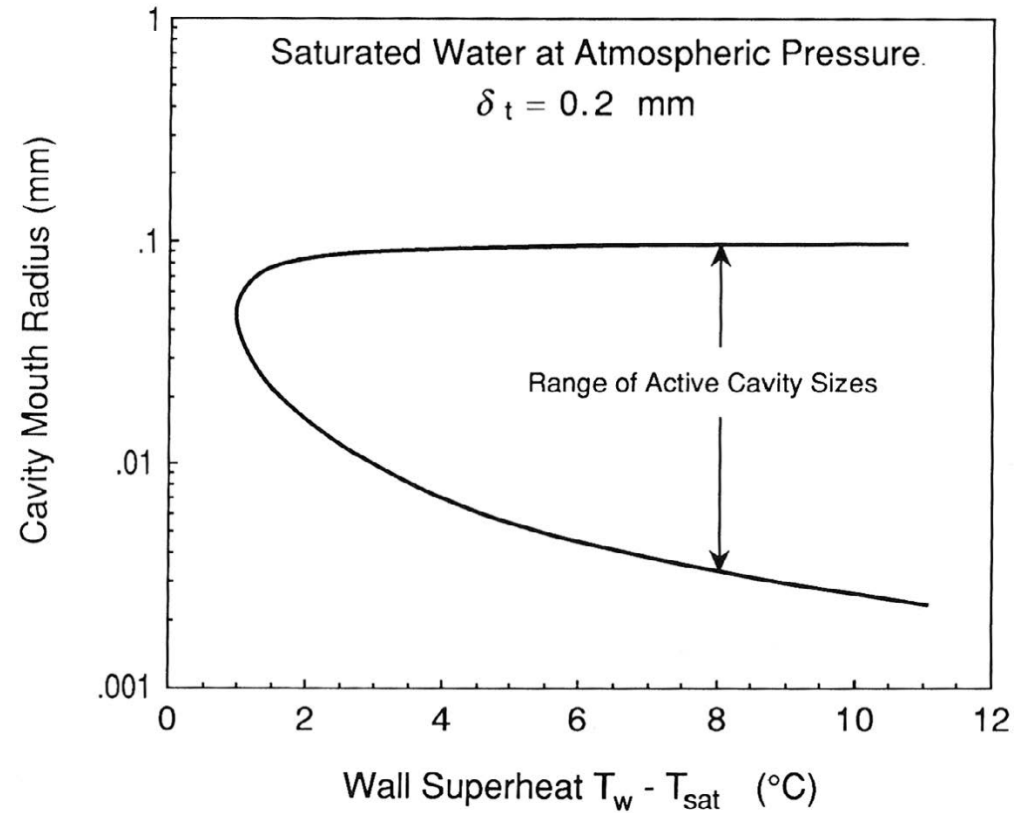
When wall superheat is less than required for onset of nucleation, no vaporization takes place

Higher superheat: subcooled liquid \rightarrow subcooled boiling \rightarrow saturated boiling dominated \rightarrow convective flow boiling \rightarrow mist evaporation \rightarrow pure vapor

Very high superheat may lead to transition boiling/film boiling near the entrance

Flow boiling device generally should operate at relatively low superheats to avoid transition/film boiling

Onset of Boiling (Hsu's Model)



- Range of active nucleation site is determined by
 - Thermal boundary layer thickness
 - Subcooling
 - Wall superheat

Boundary layer thickness implies heat flux

- Energy balance for the single-phase regime $q'' = h_{le}[T_w(z) - T_l(z)]$

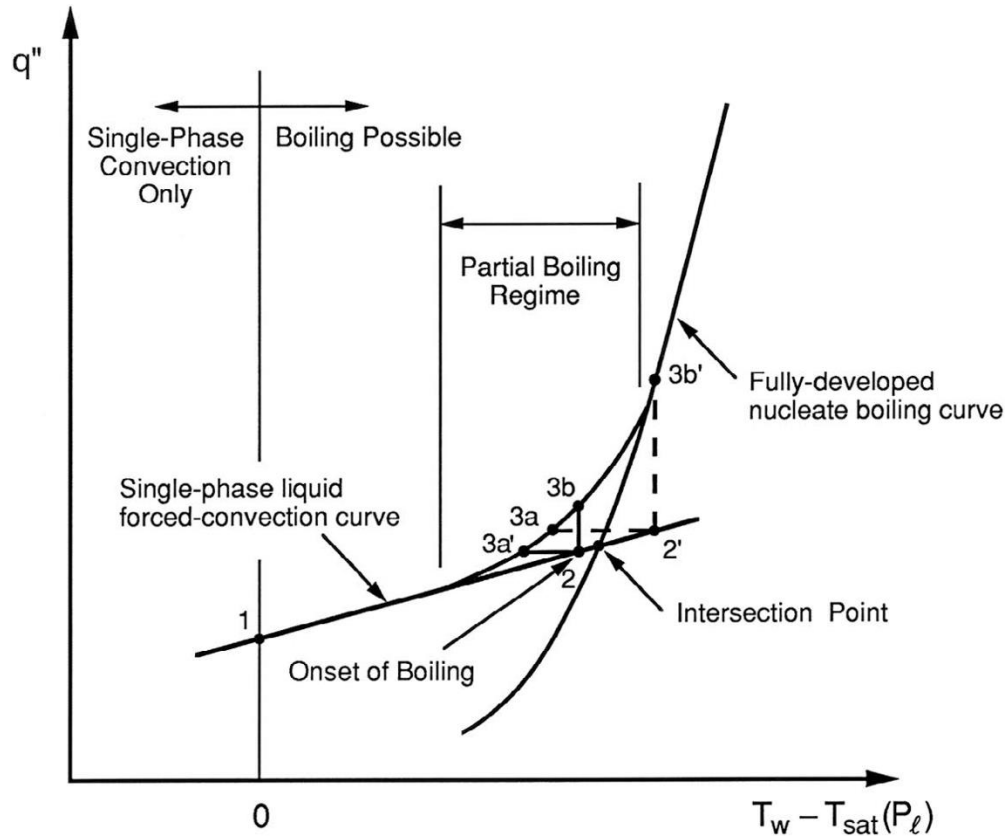
Constant wall heat flux condition
(a cylindrical tube with diameter d_h)

$$q'' = c_{pl}G[T_l(z) - T_{l,in}] \frac{\pi d_h^2}{4} = c_{pl}G[T_l(z) - T_{l,in}] \left(\frac{d_h}{4z} \right)$$

$$T_w(z) - T_{sat} = \frac{q''}{h_{le}} \left[1 + \frac{4h_{le}z}{Gc_{pl}d_h} \right] - (T_{sat} - T_{l,in})$$

q'' : wall heat flux
 z : position along the tube (inlet: $z = 0$)
 $T_l(z)$: bulk liquid temperature at z

G : mass flux in the tube
 d_h : hydraulic diameter
 c_{pl} : specific heat of liquid



Full-developed nucleate boiling

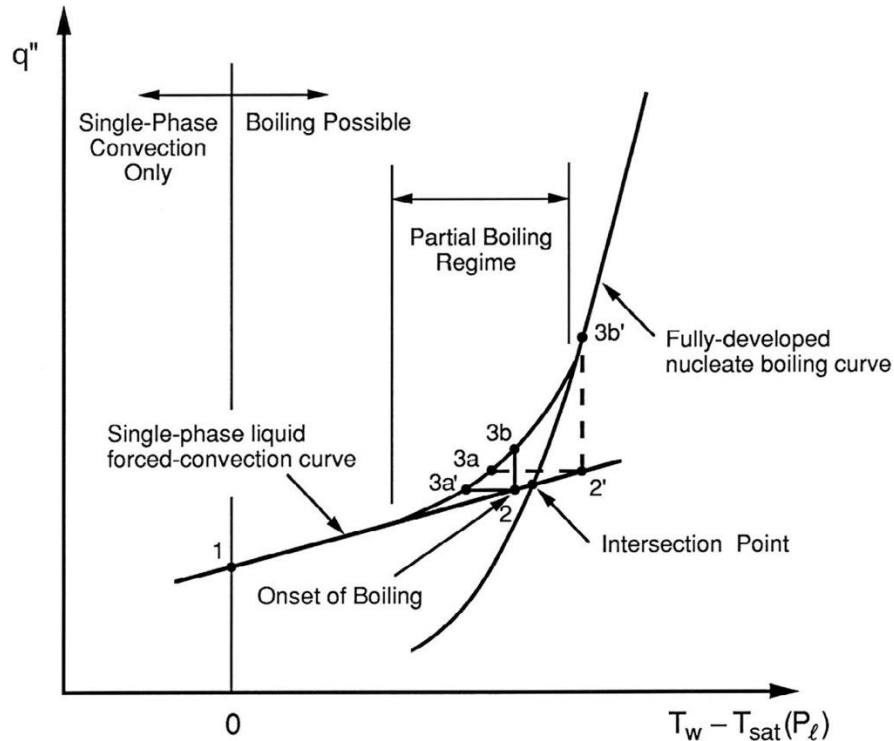
$$q'' = \gamma (T_w - T_{sat}(P_l))^m$$

γ : a factor that depends on surface and fluid properties

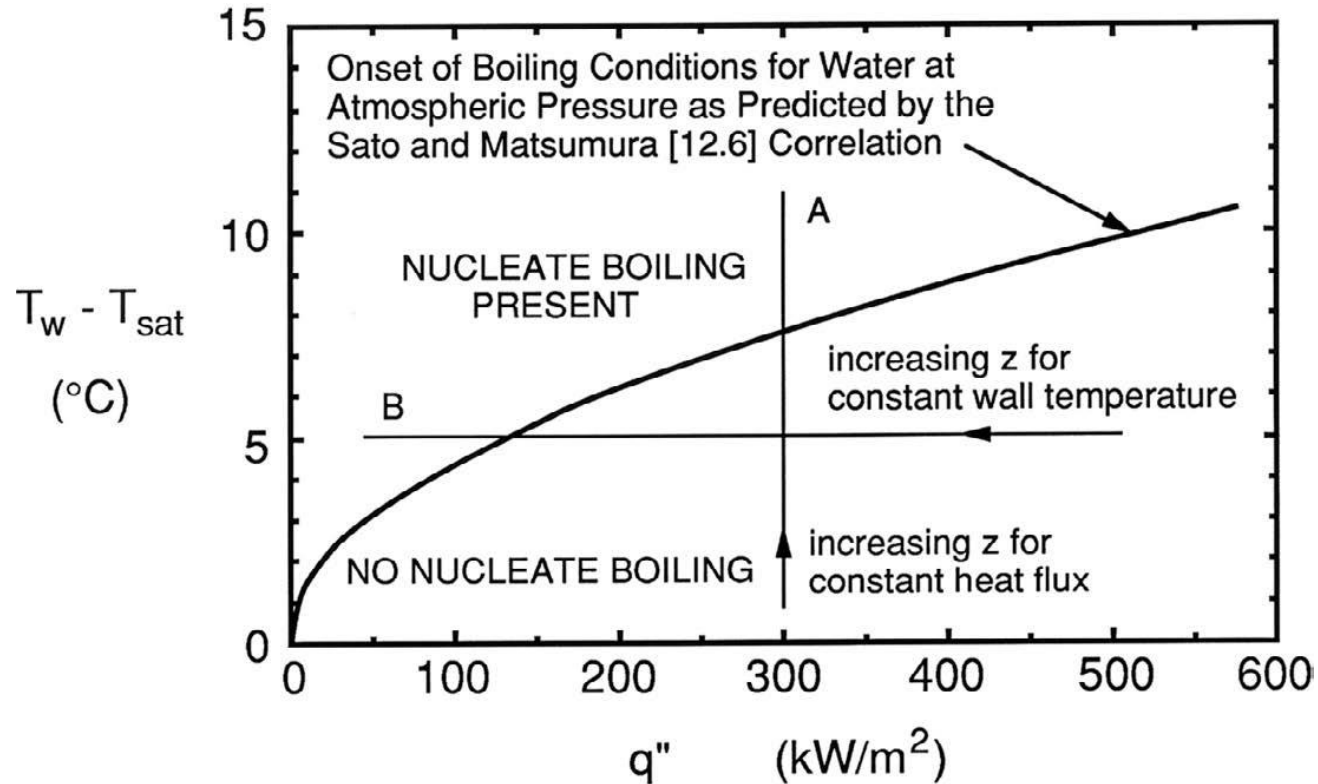
m : empirically determined, typically between 2 and 4

At intersection point

$$\left(\frac{q''}{\gamma}\right)^{1/m} = \frac{q''}{h_{le}} \left[1 + \frac{4h_{le}z}{Gc_{pl}d_h} \right] - (T_{sat} - T_{l,in})$$



- The onset may occur either before or after the intersection of the single-phase curve with the fully developed boiling curve.
- If the onset occurs at point 2, and the heat flux is held constant, the operating point may jump horizontally to point 3a'.
- If the transition is delayed to point 2', the operating point may jump horizontally to point 3a.



Correlation provided by Sato and Matsumura

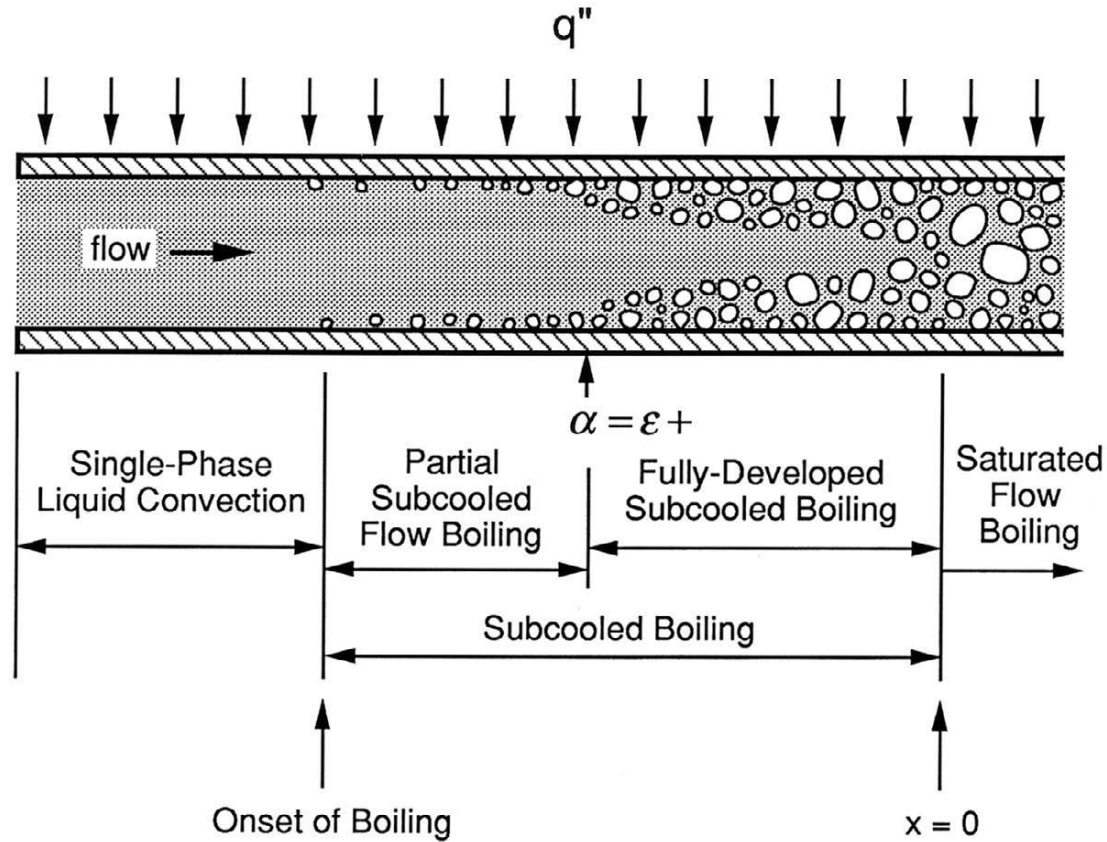
Eq. 12.14 in Carey

$$q''_{ONB} = \frac{k_l h_{lv} \rho_v}{8\sigma T_{sat}} [(T_w - T_{sat})_{ONB}]^2$$

Energy balance for the single-phase regime

$$T_w(z) - T_{sat} = \frac{q''}{h_{le}} \left[1 + \frac{4h_{le}z}{Gc_{pl}d_h} \right] - (T_{sat} - T_{l,in})$$

Subcooled Flow Boiling



- **Partial** boiling: vapor present only very near the wall
- **Fully-developed** boiling: vapor exists in a significant portion of the bulk flow near the wall

- Particularly interesting for high-heat-flux cooling

- Rohsenow's postulation (Eqs. 12.26 and 12.27 in Carey)

Total heat flux $q'' = q''_{spl} + q''_{snb}$

Single phase contribution $q''_{spl} = h_{le} [T_w - T_l(z)]$

Nucleate boiling contribution

$$\frac{q''_{snb}}{\mu_l h_{lv}} \left[\frac{\sigma}{g(\rho_l - \rho_v)} \right]^{1/2} = \left(\frac{1}{C_{sf}} \right)^{1/r} \text{Pr}_l^{-s/r} \left[\frac{c_{pl} [T_w - T_{sat}(P_l)]}{h_{lv}} \right]^{1/r}$$

Saturated Flow Boiling

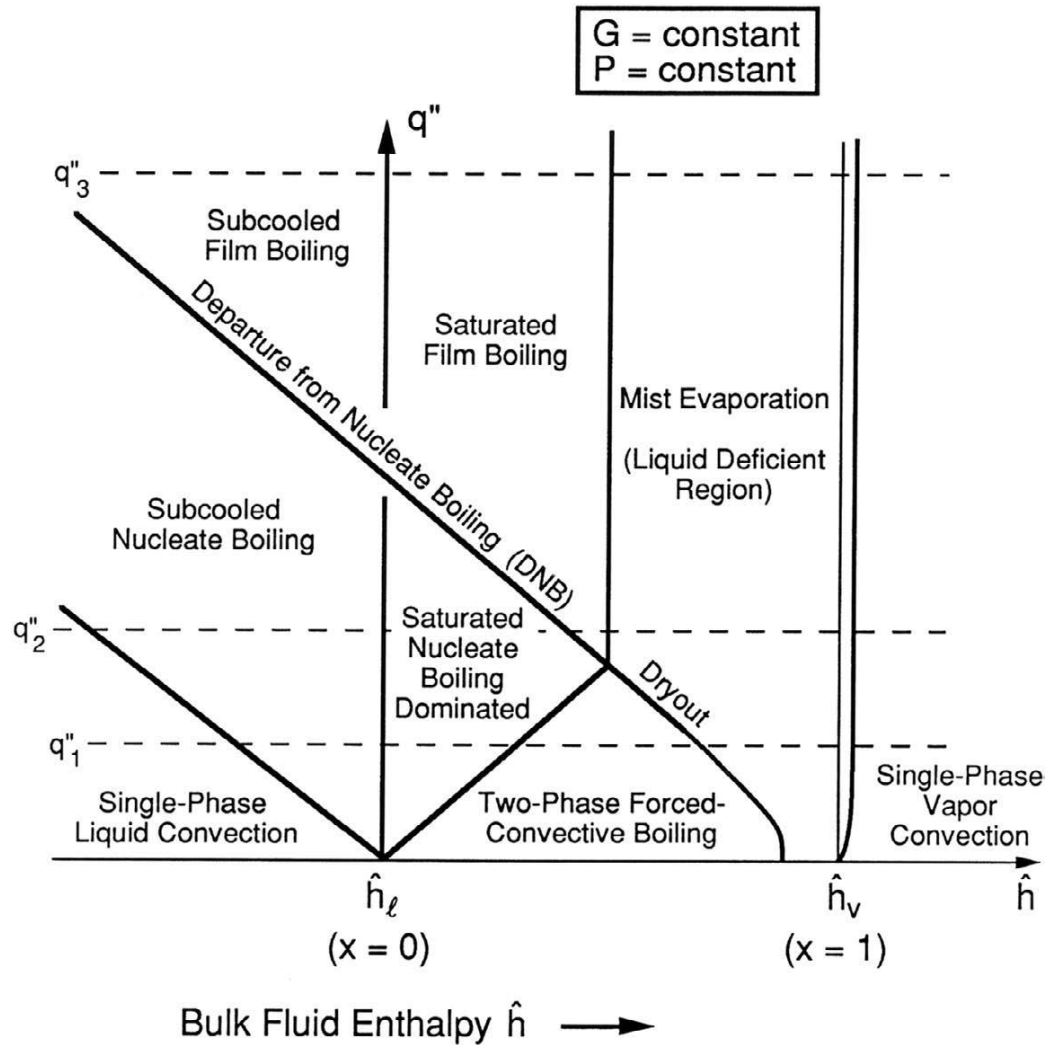


Figure 12.4 in Carey

- Saturated flow boiling is most often encountered in applications where complete or nearly complete vaporization of the coolant is desired.
- Applications:
 - evaporator of refrigeration and air-conditioning systems
 - cryogenic processing
 - boilers in power plants

- Gungor and Winterton correlation (upflow vertical tubes, diameter D)

$$h = h_l \left[1 + 3000 \left(\frac{q''}{G h_{lv}} \right)^{0.86} + \left(\frac{x}{1-x} \right)^{0.75} \left(\frac{\rho_l}{\rho_v} \right)^{0.41} \right]$$

$$h_l = 0.023 \left(\frac{k_l}{D} \right) \text{Re}_l^{0.8} \text{Pr}_l^{0.4} \quad \text{Liquid phase convective HTC}$$

$$\text{Re}_l = \frac{G(1-x)D}{\mu_l} \quad \text{Liquid phase Reynolds number}$$

- Kandlikar's Correlation

$$h = \max\{h_{NBD}, h_{CBD}\}$$

h_{NBD} : HTC for nucleate boiling dominant regime

h_{CBD} : HTC for convective boiling dominant regime

$$h_{NBD} = 0.6683 \left(\frac{\rho_l}{\rho_v} \right)^{0.1} x^{0.16} (1-x)^{0.64} f_2(\text{Fr}_{le}) h_{le} + 1058 \left(\frac{q''}{G h_{lv}} \right)^{0.7} F_K (1-x)^{0.8} h_{le}$$

$$h_{CBD} = 1.1360 \left(\frac{\rho_l}{\rho_v} \right)^{0.45} x^{0.72} (1-x)^{0.08} f_2(\text{Fr}_{le}) h_{le} + 667.2 \left(\frac{q''}{G h_{lv}} \right)^{0.7} F_K (1-x)^{0.8} h_{le}$$

- Kandlikar's Correlation (continued)

$$\begin{aligned}
 h_{NBD} &= 0.6683 \left(\frac{\rho_l}{\rho_v} \right)^{0.1} x^{0.16} (1-x)^{0.64} f_2(\text{Fr}_{le}) h_{le} \\
 &+ 1058 \left(\frac{q''}{G h_{lv}} \right)^{0.7} F_K (1-x)^{0.8} h_{le}
 \end{aligned}$$

$\text{Fr}_{le} = \frac{G^2}{\rho_l^2 g D}$, Froude number comparing inertial force to buoyance force

TABLE 12.1

Fluid Constant Values for the Kandlikar [12.53] Correlation

Fluid	F_K
Water	1.00
R-11	1.30
R-12	1.50
R-13B1	1.31
R-22	2.20
R-113	1.30
R-114	1.24
R-134a	1.63
R-152a	1.10
Nitrogen	4.70
Neon	3.50

$$f_2(\text{Fr}_{le}) = \begin{cases} (25\text{Fr}_{le})^{0.3} & \text{for } \text{Fr}_{le} < 0.04 \text{ with horizontal tubes} \\ 1 & \text{for } \text{Fr}_{le} > 0.04 \text{ with horizontal tubes and for all vertical tubes} \end{cases}$$

- Kandlikar's Correlation (continued)

$$h_{NBD} = 0.6683 \left(\frac{\rho_l}{\rho_v} \right)^{0.1} x^{0.16} (1-x)^{0.64} f_2(\text{Fr}_{le}) h_{le} + 1058 \left(\frac{q''}{G h_{lv}} \right)^{0.7} F_K (1-x)^{0.8} h_{le}$$

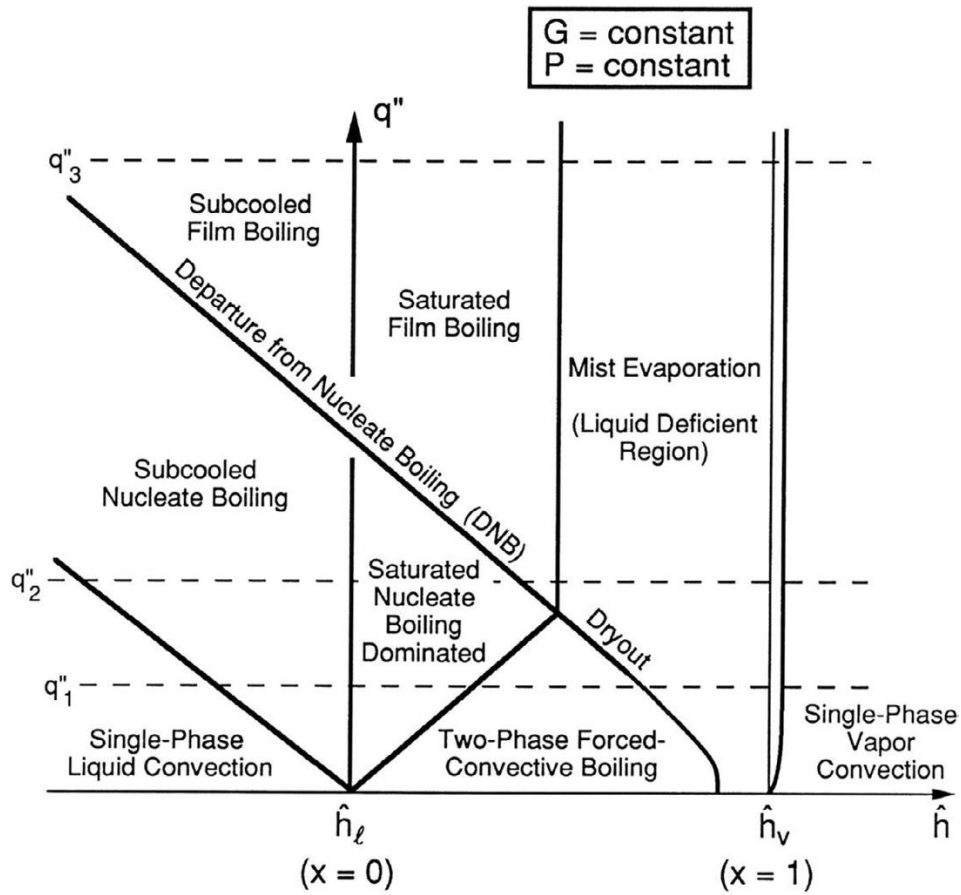
$$h_{CBD} = 1.1360 \left(\frac{\rho_l}{\rho_v} \right)^{0.45} x^{0.72} (1-x)^{0.08} f_2(\text{Fr}_{le}) h_{le} + 667.2 \left(\frac{q''}{G h_{lv}} \right)^{0.7} F_K (1-x)^{0.8} h_{le}$$

$$0.5 \leq \text{Pr}_l \leq 2000 \text{ and } 2300 \leq \text{Re}_{le} < 10^4: \quad h_{le} = \left(\frac{k_l}{D} \right) \frac{(\text{Re}_{le} - 1000) \text{Pr}_l (f/2)}{1 + 12.7 (\text{Pr}_l^{2/3} - 1) (f/2)^{0.5}}$$

$$0.5 \leq \text{Pr}_l \leq 2000 \text{ and } 10^4 \leq \text{Re}_{le} \leq 5 \times 10^6: \quad h_{le} = \left(\frac{k_l}{D} \right) \frac{\text{Re}_{le} \text{Pr}_l (f/2)}{1.07 + 12.7 (\text{Pr}_l^{2/3} - 1) (f/2)^{0.5}}$$

$$f = [1.58 \ln(\text{Re}_{le}) - 3.28]^{-2} \quad \text{Re}_{le} = GD/\mu_l$$

Critical Heat Flux Condition (Departure from Nucleate Boiling)



Bulk Fluid Enthalpy \hat{h} →

Figure 12.4 in Carey

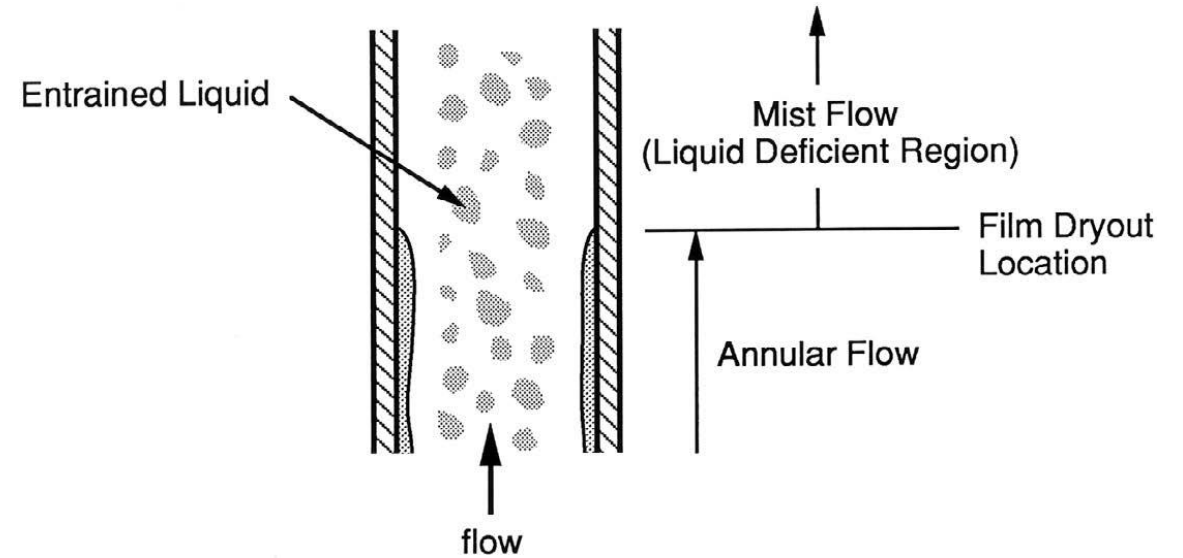
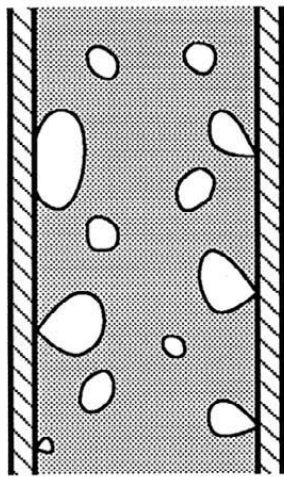


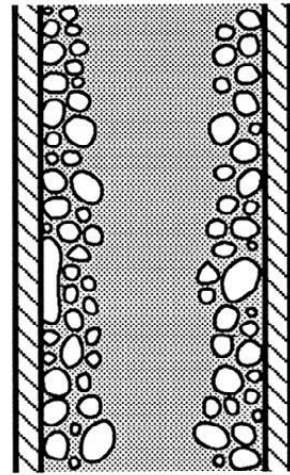
Figure 12.18 in Carey

Dry-Out Mechanisms (Hypotheses)



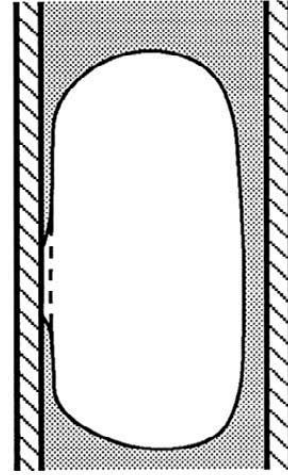
Dryout Under a
Growing Bubble

(a)



Vapor Crowding

(b)



Dryout Under
a Vapor Slug

(c)

(a) Liquid microlayer underneath the bubble evaporates faster than it can be replenished

(b) Near wall regime filled with vapor pockets, hindering liquid flow

(c) When a slug passes a heated section, the thin film completely evaporates before slug passes

Figure 12.19 in Carey

- Subcooled case: Celata's correlation

$$\frac{q''_{crit}}{Gh_{lv}} = \frac{C_c}{Re_{le}^{0.5}} \quad Re_{le} = \frac{GD}{\mu_l}$$

$$C_c = (0.216 + 0.0474P)\Psi \quad P: \text{local pressure in MPa}$$

$$\Psi = \begin{cases} 1 & \text{for } x_{out} < -0.1 \\ 0.825 + 0.986x_{out} & \text{for } -0.1 < x_{out} < 0 \end{cases}$$

$$x_{out} = \frac{c_{pl}(T_{l,out} - T_{sat})}{h_{lv}} \quad \text{Recommended for } P \leq 5.5 \text{ Mpa, } G/\rho_l \text{ of 2.2-40 m/s, } T_{sat} - T_{l,out} \text{ of 15-190 K, } 0.3 \text{ mm} \leq D \leq 15 \text{ mm}$$

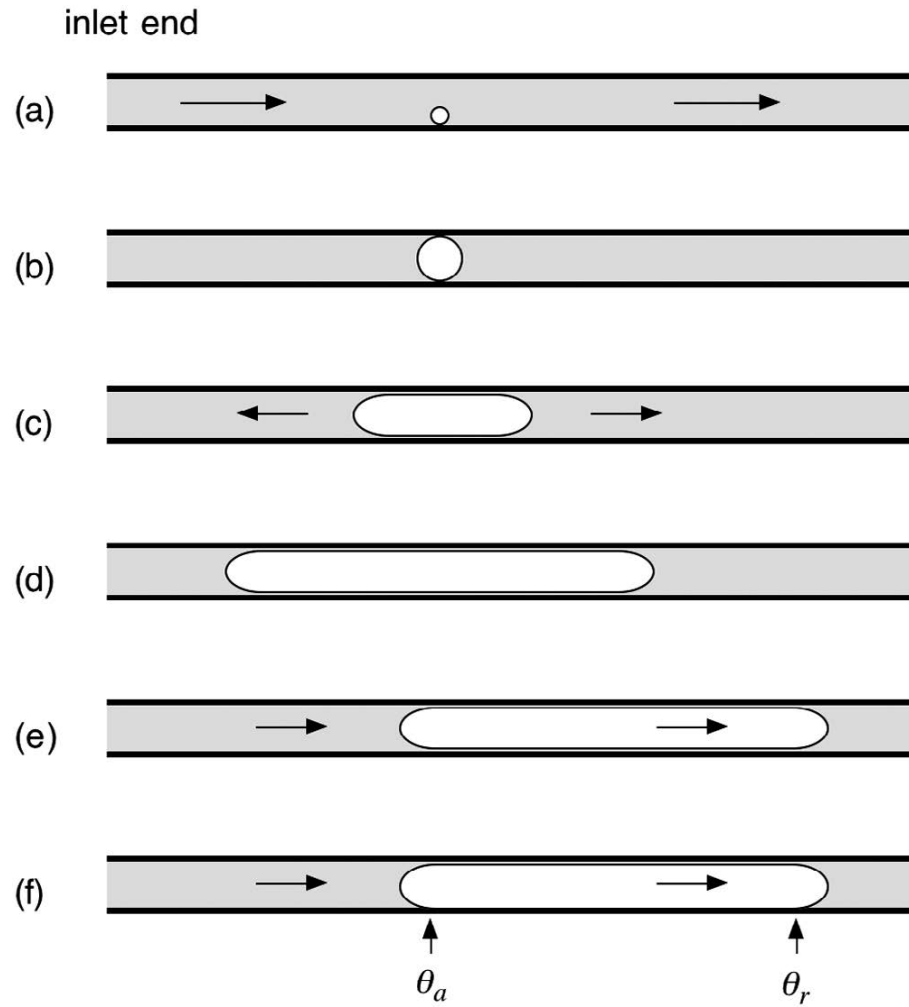
- Saturated case: “The 2006 CHF look-up table” by Groeneveld *et al.*

Pressure [kPa]	Mass Flux [kg m ⁻² s ⁻¹]	CHF [kW m ⁻²]																							
		X→ -0.50	-0.40	-0.30	-0.20	-0.15	-0.10	-0.05	0.00	0.05	0.10	0.15	0.20	0.25	0.30	0.35	0.40	0.45	0.50	0.60	0.70	0.80	0.90	1	
100	0	8111	7252	6302	4802	4086	3057	1990	1142	637	415	284	223	188	165	152	142	133	123	114	110	96	55	0	
100	50	8317	7271	6326	5035	4236	3453	2420	1570	1011	784	641	587	553	531	475	443	419	387	347	277	239	204	0	
100	100	8390	7295	6371	5322	4586	3640	2942	2103	1558	1275	1013	885	847	811	789	758	745	715	700	600	459	359	0	
100	300	10698	9288	7795	6020	5009	3865	3196	2479	1961	1707	1317	1177	1172	1159	1150	1100	1085	1041	1031	675	517	366	0	
100	500	12882	10946	9224	6791	5348	3938	3369	2685	2087	1808	1412	1347	1311	1303	1282	1260	1212	1193	1071	605	450	295	0	
100	750	16982	14405	11641	7496	5662	4234	3471	2780	2229	1970	1649	1606	1591	1563	1510	1495	1400	1280	595	415	243	206	0	
100	1000	19441	16278	13255	8232	5971	4495	3533	3012	2653	2349	2070	2000	1980	1930	1715	1550	1359	1165	503	322	172	105	0	
100	1500	22781	19225	15465	9100	6603	5358	3741	3524	3166	2917	2635	2572	2467	2378	1908	1350	1005	815	302	210	126	51	0	
100	2000	25268	21321	17143	9141	7059	6036	4074	3855	3556	3402	3167	2986	2720	2549	1696	1105	805	595	247	105	87	39	0	
100	2500	28026	23599	18346	9503	7506	6516	4502	4047	3852	3599	3228	3019	2676	2458	1148	956	708	465	290	120	46	22	0	
100	3000	30294	25465	19383	9779	8063	7088	4826	4182	3976	3389	2968	2706	2369	1829	940	846	665	532	302	159	55	20	0	
100	3500	32227	27043	21068	10156	8518	7302	5113	4384	4106	3196	2769	2557	2311	1729	1158	891	817	670	402	210	75	28	0	
100	4000	33928	28471	22722	10512	8728	7528	5582	4709	4228	3119	2736	2504	2282	1850	1470	1160	1030	823	475	248	96	38	0	
100	4500	35406	29774	23890	10945	9088	8067	6267	5013	4272	3287	2789	2541	2304	1972	1718	1405	1185	969	585	289	129	61	0	
100	5000	36808	30988	24979	11185	9592	8576	6748	5113	4342	3410	2890	2629	2355	2066	1779	1498	1247	1030	647	347	167	81	0	
100	5500	38232	32141	25791	11929	10084	8940	6867	5175	4389	3465	2954	2680	2406	2128	1848	1595	1334	1118	729	409	206	101	0	
100	6000	39525	33222	26637	13026	10396	9347	6919	5241	4423	3580	2921	2681	2447	2170	1908	1651	1418	1204	807	468	244	121	0	
100	6500	40727	34244	27480	14371	10748	9701	6995	5295	4491	3620	2918	2694	2477	2209	1965	1719	1493	1281	878	523	282	142	0	
100	7000	41950	35224	28165	15045	11091	10522	7062	5370	4513	3668	2958	2724	2501	2247	2013	1780	1559	1349	943	576	319	162	0	
100	7500	43448	36075	28604	15822	11538	10726	7087	5381	4585	3699	2996	2751	2526	2285	2060	1838	1622	1414	1000	615	347	180	0	
100	8000	44338	36803	29089	16599	12085	10900	7313	5392	4689	3780	3031	2778	2553	2320	2103	1890	1679	1473	1054	651	371	196	0	

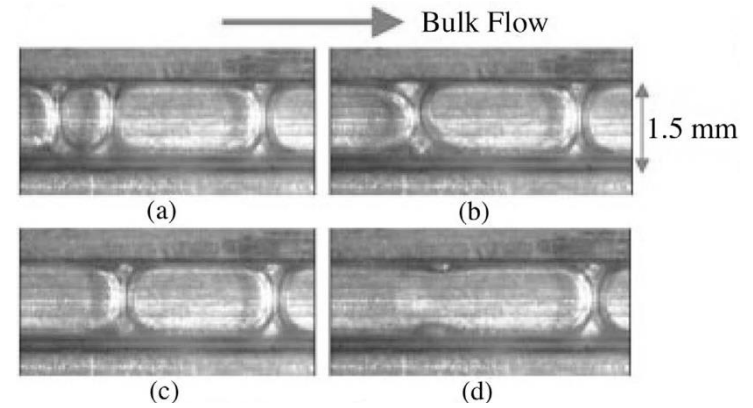
<https://doi.org/10.1016/j.nucengdes.2007.02.014>

https://github.com/greenwoodms06/2006_Groeneveld_CriticalHeatFlux_LUT

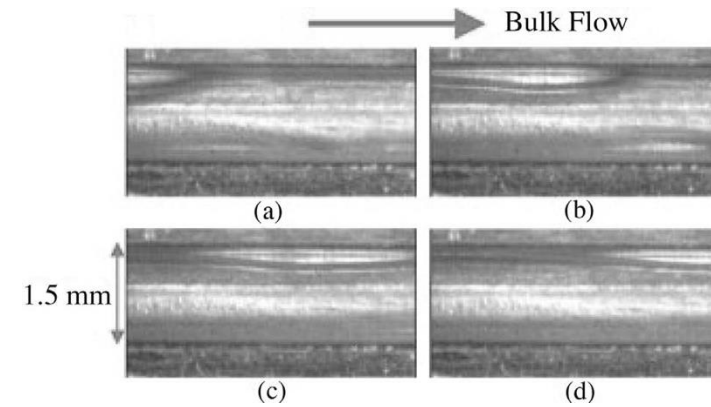
Flow Boiling in Microchannels



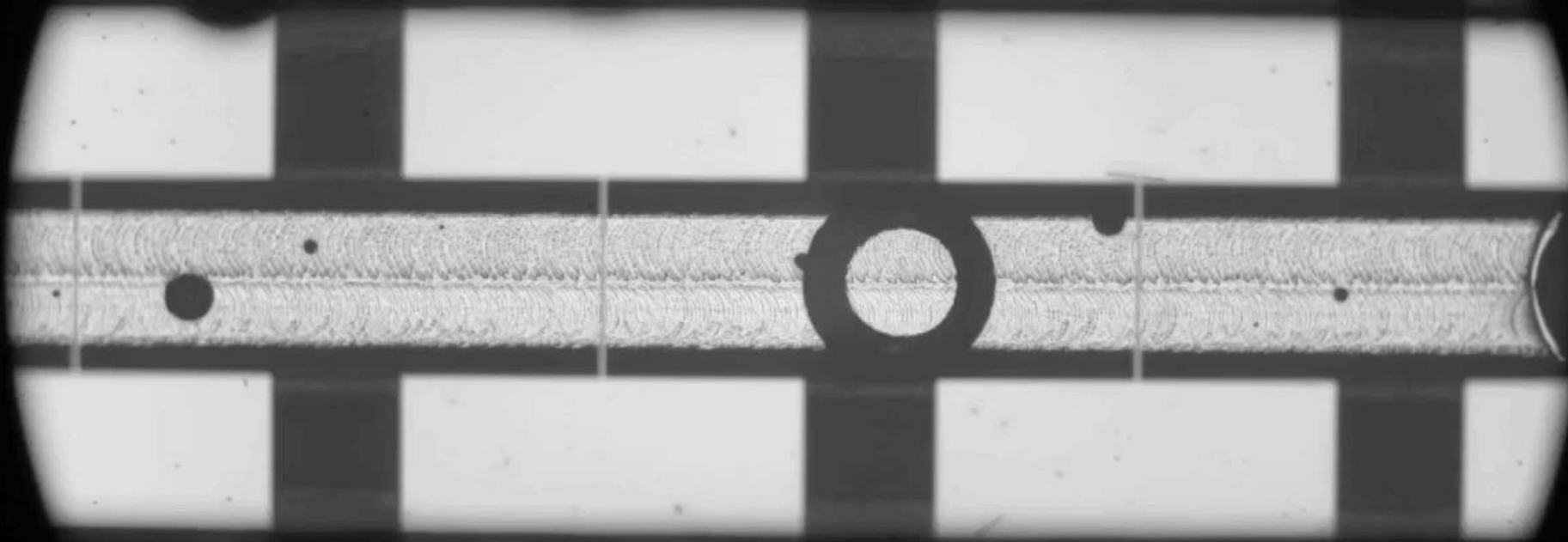
Slug flow



Annular flow



Vapor Backflow Instability



60 fps; real time duration: 210 ms

Credit: Mark
Schepperle